JOURNAL OF GEOPHYSICAL RESEARCH, VOL. 94, NO. B11, PAGES 15,771–15,784, NOVEMBER 10, 1989

Paleointensity of the Geomagnetic Field From Dated Lavas of the Chaîne des Puys, France 1. 7–12 Thousand Years Before Present

JEAN-SÉBASTIEN SALIS AND NORBERT BONHOMMET

Laboratoire de Géophysique Interne, Université de Rennes I, France

SHAUL LEVI

College of Oceanography, Oregon State University, Corvallis

Paleointensities were determined by the Thellier method for six dated lava flows from the Chaîne des Puys (France), with ages from 7 to 12 ka (ka = kiloannum before present). The three younger flows overlap the archaeomagnetic period for Europe, and the older flows extend the record to more ancient times. Our results support the quasi-sinusoidal variation of the geomagnetic field intensity since 10 ka for Europe, punctuated by a peak virtual dipole moment of about 11×10^{22} A m^2 between 8 and 10 ka; the data from 10 to 12 ka show considerably lower virtual dipole moments between 4 and 5×10^{22} A m^2, about 60% of the global average since 10 ka. When compared with available worldwide data, the maximum in the virtual dipole moment between 8 and 10 ka is supported by measurements from Japan and possibly Hawaii. Lower than average virtual dipole moments between 10 and 12 ka have also been observed in North America and Hawaii. The existing data suggest that from 8 to 10 ka the geomagnetic field supported a dipole moment up to 30% above and from 10 to 12 ka about 30% below the average value since 10 ka.

INTRODUCTION

Paleomagnetic studies of dated, in situ volcanic rocks and archaeological materials can provide a complete vector description of the Earth's magnetic field as a function of time. This information contributes to the knowledge of geomagnetic variations and ultimately to understanding the geodynamo.

Thermoremanent magnetization (TRM) is the only remanence that can be used to determine absolute paleointensities, because it can be reproduced in the laboratory and the controlling physical processes are relatively well understood. TRM is usually acquired parallel to the ambient field, as the magnetic grains cool from above their Curie points to below the blocking temperature, and TRM intensity is generally linearly proportional to the inducing geomagnetic field. To be useful for geomagnetism, the time of TRM acquisition must be known. Considerable paleointensity results have been obtained for historical and Holocene time from different parts of the world: For example, Europe [*Thellier and Thellier*, 1959; *Kovacheva and Veljovich*, 1977; *Kovacheva*, 1980, 1982; *Schweitzer and Soffel*, 1980; *Walton*, 1979, 1984; *Aitken et al.*, 1985], Egypt [*Games*, 1977, 1980; *Aitken et al.*, 1984; *Athavale*, 1969], United States [*Bucha et al.*, 1970; *Champion*, 1980; *Sternberg*, 1983], Japan [*Nagata et al.*, 1963; *Kitazawa*, 1970; *Tanaka*, 1980]. However, the bulk of paleointensity data is from Europe. Analyses of worldwide data [*Barton et al.*, 1979; *McElhinny and Senanayake*, 1982] have been used in an effort to isolate variations of the dipole moment from those of the total field intensity. To do this, the paleointensities were transformed to virtual dipole moments (VDM) and/or to virtual axial dipole moments (VADM) depending on whether the inclination was or was not known, respectively, thus averaging out nondipole components from different parts of the world. These data compilations show a quasi-sinusoidal variation of the intensity over Europe for the period from the present to 8 ka (ka = thousand years before present) [*Barton et al.*, 1979], first pointed out by *Cox* [1968]. However, the amplitude of the "sine function" is diminished by global averaging [*McElhinny and Senanayake*, 1982]. Therefore it is possible that this "sinusoidal" variation is not a worldwide feature, but rather it is biased by the European results. A better global distribution and especially more data from the southern hemisphere are needed to resolve the dipole and nondipole contributions to the secular variation of the paleomagnetic intensity.

The considerable Holocene data are mostly from stable TRM in archaeological artifacts, such as potteries, tiles, bricks, etc., which acquired their TRM on cooling in air from temperatures well above the Curie points of their magnetic minerals, thus recording the geomagnetic direction and intensity. Because the original heatings were in air, further chemical changes of the magnetic minerals would be minimized during subsequent laboratory heatings in air. Another advantage of archaeological materials is that they can often be accurately dated. Very few archaeological artifacts are available prior to about 8 ka, and the TRM of dated lavas provides the most suitable source for extending the time series of vector description of the paleomagnetic field.

In this paper we present paleointensity determinations of six lavas from the Chaîne des Puys in central France, dated by the thermoluminescence (TL) method performed on feldspars [*Guérin*, 1983], with ages between 7 and 12 ka. The flows and their estimated ages are shown on Figure 1. Results from the three units with ages younger than 10 ka will be compared with the archaeomagnetic record from Europe to provide a test of our experimental procedures, to demonstrate the suitability of these volcanic rocks for reliable paleointensity determinations, and to add confidence in the TL dating of these flows. The three older lavas extend the paleointensity variations for Europe beyond the Holocene period, for which only few data are presently available.

METHODS

Paleointensities were obtained by the Thellier method [*Thellier and Thellier*, 1959] modified by *Coe* [1967*a*,*b*]. The primary difficulty with paleointensity experiments is that most rocks

Paper number 89JB01086.
0148-0227/89/89JB-01086$05.00

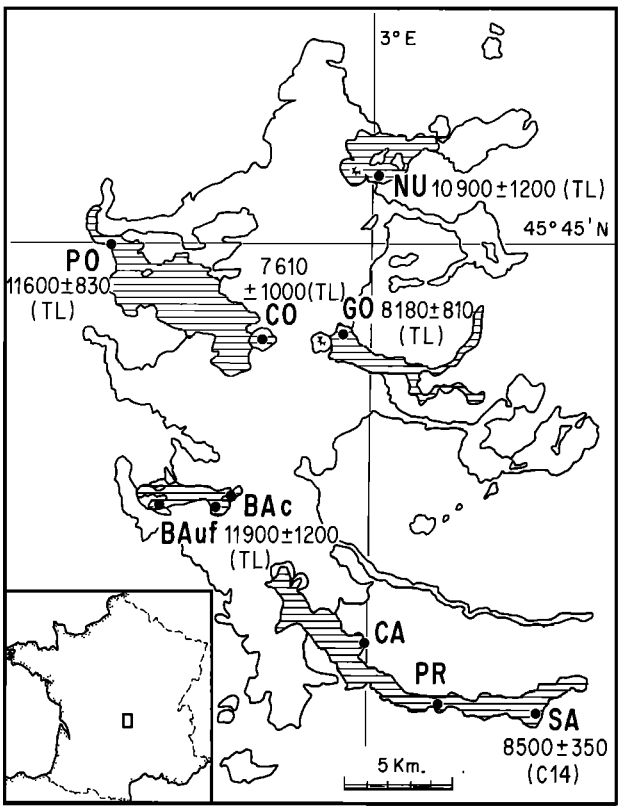

Fig. 1. Location map of the Chaîne des Puys, France. The shaded regions indicate the extent of the volcanic units of this study. Solid dots refer to sampling sites; the numbers correspond to age estimates and associated uncertainties in years before present; dating method is also shown (TL, thermoluminescence; C14, radicarbon).

undergo chemical alteration of their magnetic properties when heated beyond a certain temperature, and then they are no longer suitable for paleointensity determinations. The chief advantage of the Thellier double heating procedure is that the temperature is increased progressively in steps from room temperature to the maximum blocking temperature. Assuming the natural remanent magnetization (NRM) is essentially TRM and if the partial TRMs (PTRMs) are independent and additive, then each temperature step provides a unique paleointensity determination. This method often enables detection of the onset temperature of significant chemical changes, which preclude further use of the specimen for paleointensity studies. Changes of the magnetic properties are frequently accompanied by irreversible modification of PTRM acquisition which are often detected by deviations from linearity of the partial NRM (PNRM) versus PTRM plot.

In our experiments, extensive use was made of PTRM checks to assess the samples' integrity for paleointensity determinations. The PTRM check consists of repeating the PTRM acquisition at an intermediate temperature T_i after that temperature had been equaled or exceeded by the double heating Thellier procedure. The PTRM check tests whether the PTRM acquired between T_i and room temperature is the same even after the specimen had been heated to a temperature $T \geq T_i$. Any difference between the two PTRMs indicates that some magnetic change had occurred. Only the temperature range with "successful" PTRM checks can be considered unaltered for purposes of paleointensity determinations. Because in the Thellier procedure each paleointensity determination is based on several temperature steps and because it enables earlier detection of magnetochemical changes, Thellier's method appears to be the most reliable for paleo-intensity determinations of volcanic rocks [see also *Coe and Grommé*, 1973].

MEASUREMENTS AND EXPERIMENTAL PROCEDURE

Khodair and Coe [1975] showed that for basaltic rocks, high-temperature alteration of the magnetic properties is minimized during vacuum heatings, yielding more accurate paleointensity results. Therefore, in our experiments, samples were usually heated in an evacuated quartz tube at pressures less than 10^{-2} torr. Specimens of highly oxidized scoria were heated in air. Following *Levi* [1975], the field producing the PTRM was applied during the entire temperature cycle. To produce the laboratory field, we constructed a coil surrounding the quartz tube and shielded from the Earth's field by three layers of nested μ-metal cylinders. Each heating cycle (with six samples in the tube) lasted at least 90 min; the furnace reached the desired temperature after a half hour. The cooling time was usually about 75 min. All remanence measurements were made at room temperature on a spinner magnetometer. At each temperature step the first measurement was the PNRM left after heating and cooling in zero field. The second measurement was the vector sum of the remaining PNRM and the PTRM acquired after heating and cooling to the same temperature in the laboratory field. Vector subtraction gave values of PNRM lost and PTRM acquired.

With increasing temperature during the Thellier procedure, the temperature of the PTRM checks was also increased, because it is possible that certain mineralogic changes might not alter minerals with low blocking temperature, while significantly affecting particles with higher blocking temperatures. Although the PTRM check is the best known test for the reliability of paleointensity results, a "good" PTRM check is not sufficient to assure a correct paleointensity. Sometimes magnetochemical changes can occur which are not detectable by PTRM checks [*Prévot et al.*, 1983]. Examples of such behavior arise when the blocking tempe-ratures of the affected grains are higher than the step temperature.

SELECTION CRITERIA

The Thellier method is very time consuming, and there are many lavas that are not suitable for paleointensity determination. Such nonsuitability is usually expressed by nonideal behavior in the Thellier experiment, that is, nonlinear NRM-TRM curves. To maximize the success of the paleointensity experiments, several laboratory procedures were used to guide the sample selection for the Thellier experiments. Samples were chosen (1) to have NRM with minimum secondary overprinting, (2) to be composed of more oxidized iron titanium oxides with higher Curie points and with near reversible saturation magnetization versus temperature curves, and (3) to have stable remanence in predominantly single and pseudo-single domain grains.

Samples for the paleointensity experiments were selected to have NRMs with minimum secondary remanence components, such as viscous remanent magnetization (VRM) and isothermal RM (IRM). These secondary remanences often cause nonlinearities in the lower-temperature points of the NRM-TRM diagrams. Lightning effects are often easily recognized, because they frequently produce high and variable NRM intensities and scattered directions. The primary remanence direction of each site was determined by stepwise alternating field (AF) demagnetization of one specimen from each oriented core from the studied units. Samples for paleointensity studies were selected from those with NRM directions similar to the stable site mean direction.

However, because these young lavas cooled in a normal polarity field, secondary VRM produced in the Holocene would be subparallel to the original TRM and might have a negligible effect on the scatter of remanence directions. Therefore a storage test was performed to evaluate the viscosity index. Samples from the six flows were oriented parallel and antiparallel to the ambient field for 10 days. The calculated viscosity index never exceeded 5% of the total NRM, indicating that the studied lavas are relatively free of viscous magnetization. The small calculated VRM components might represent experimental errors, as indicated by their randomly distributed directions.

Samples for the paleointensity experiments were preferentially selected to have more highly oxidized titanomagnetite minerals, because such samples are less susceptible to further chemical changes during subsequent laboratory heatings. Alteration of the magnetic properties during heatings of the Thellier experiment is probably the most common cause for nonideal behavior and the major cause for aborted (rejected) paleointensity determinations. These physical/chemical changes become more pronounced at elevated temperatures. Saturation magnetization (J_s) versus temperature (T) was measured in vacuum for each core used for the paleointensity determinations, using an automated Curie balance. To minimize the effects of alteration of the magnetic properties upon heating, whenever possible, samples for the paleointensity experiments were selected from cores with single Curie points (T_c) whose J_s-T curves were nearly reversible. Single Curie points indicate the presence of a single titanomagnetite phase, and reversibility suggests that minimum changes would be expected during the Thelliers' method sequential heating. Experience in many laboratories has shown that the best results are obtained for oxidized titanomagnetites with $T_c \gtrsim 500°C$. For sites with only low Curie points, successful paleointensity results were obtained for samples with moderate Curie points ($100° < T_c < 300°$ C), provided there existed a finite temperature range with reversible J_s-T behavior. An example of this will be shown later with sample SA 165.

TRM in multidomain grains can produce nonideal behavior in Thellier experiments [*Levi*, 1977], resulting in concave-up curvature of the NRM-TRM points, and paleointensities determined using only the lower-temperature NRM-TRM data would preferentially lead to overestimates due to their steeper slopes. Therefore samples dominated by multidomain remanence should be avoided whenever possible. A low viscosity index ($\lesssim$5%), lack of secondary remanence, and high remanence stability to AF demagnetization with median demagnetizing fields (MDFs) usually above 25 mT were the most important indicators that the remanence resides in single domain or pseudo-single domain particles. In this study we used these criteria, whenever possible, to reject samples with a significant fraction of remanence in multidomain grains.

EXPERIMENTAL CHECKS

During the experiments, PTRM checks were used to select the temperature intervals for determining the paleointensity, the consistency of the acquired PTRMs being a necessary (but not sufficient) condition to assure that for blocking temperatures at or below a "good" PTRM check, ideal behavior in the Thellier sense has not been violated.

An additional control on the paleointensity determination was to examine the evolution of the NRM vector during thermal demagnetization, using orthogonal vector projection diagrams. Only temperatures corresponding to the primary remanence decaying linearly to the origin were used in the paleointensity calculation. Secondary components not detected during the NRM preselection were subtracted. Scrutiny of the NRM direction during paleointensity experiments may be particularly important at high temperatures when the original magnetization might become contaminated with chemical remanence (i.e., PTRM transformed into PTCRM), acquired parallel to the laboratory field. Such behavior does not necessarily violate the linearity of the NRM-TRM plot, and the NRM-TRM diagram might fit a straight line to points which do not show any change in PTRM acquisition, while not corresponding to the primary remanence.

Two examples of rejected samples are shown in Figure 2. Sample GO 85 illustrates the usefulness of examining the direction of magnetization during the experiments. The first four points of the NRM-TRM diagram for GO 85 might have been used to obtain a paleointensity value. PTRM checks show that chemical changes of the magnetic minerals occur at higher temperatures (Figure 2*b*). However, the orthogonal projections of the remanence direction during thermal demagnetization (in sample coordinates) rotate continuously from the beginning of the demagnetization, and the original uncontaminated thermoremanence of the rock is never recovered. The first points might represent a VRM. At higher temperatures the declination remains stable, and the inclination moves toward the direction of the applied field, indicating that the sample acquires a progressively more significant TCRM (high-temperature chemical remanent magnetization). The paleointensity of sample NU 132 (Figure 2*a*) was unsuccessful despite linear (univectorial) decay to the origin of its remanence direction during thermal demagnetization. This paleointensity experiment was rejected because of

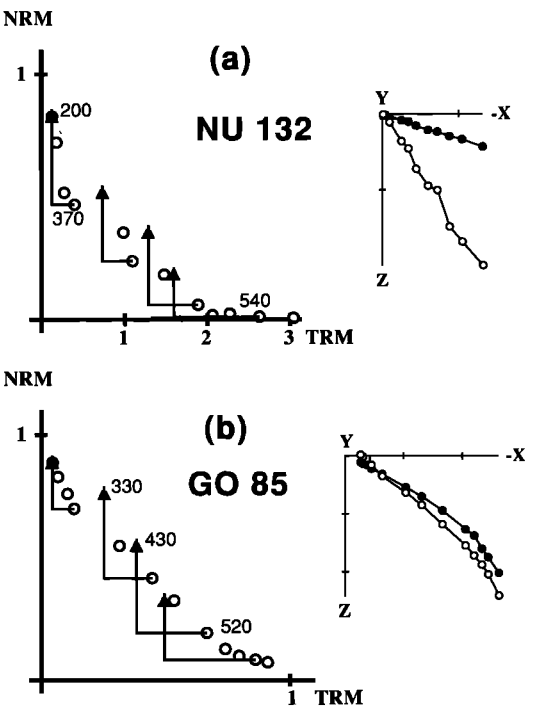

Fig. 2. Examples of rejected paleointensity determinations. NRM-TRM diagram (normalized to the original remanence) and associated orthogonal vector projections of the natural remanence during thermal demagnetization in sample coordinates. The triangles indicate the PTRM checks. The open (solid) circles in the vector diagrams represent the projection in the vertical (horizontal) plane. The laboratory field during the paleointensity experiment was vertical up.

the nonlinear NRM-TRM data and unsuccessful PTRM checks for $T>400°C$, which reflect irreversible modification in the sample's capacity of PTRM acquisition.

DATA ANALYSIS

After selection of the temperature steps, the paleointensity was calculated using least squares fitting of a straight line [*York*, 1966, 1967] through the chosen NRM-TRM points. The value of the original NRM was always excluded, because of frequent, though minor, viscous overprints. After determining the slope and the paleofield intensity, an associated quality factor q was calculated [*Coe et al.*, 1978] to estimate the reliability of each paleointensity determination. This factor depends on the NRM fraction used in the calculation, the number of points used, the dispersion of the points about the straight line, and the length of the gaps between individual points.

In this study the quality factors vary considerably between samples, due to differences in sample mineralogies, grain size distributions, and their varied responses to heatings. Because significant differences in q can occur within the same unit, the mean paleointensity for each unit (lava flow) was weighted to compensate for differences in q. *Coe et al.* [1978] proposed a method for weighting, which emphasizes paleointensity results utilizing a higher NRM fraction, even if the straight line is not so well defined. *Kono and Tanaka* [1984, 1985] showed that the use of the least squares fitting of *York* [1966, 1967], used by Coe et al., is not so well adapted for the paleointensity determination, mainly because the standard deviation of the slope does not take into account the NRM fraction used for paleointensity determination, and they prefer the method of *Williamson* [1968], who also proposed a weighting scheme. More recently, *Prévot et al.* [1985] discussed the weighting procedure used by *Coe et al.* [1978] and proposed an alternative method which appears to us more suitable, because it does not exaggerate results obtained with a large NRM fraction and is less dependent on the paleointensity value. The individual results in our study were weighted by $W_i = q_i/(N_i-2)^{1/2}$, where q_i and N_i are the quality factor and number of NRM/TRM points used to calculate the paleointensity of the ith sample, respectively.

RESULTS

Puy de Côme Crater

The youngest unit studied was the flow in the Puy de Côme volcano crater (CO) dated by thermoluminescence (TL) at 7.6 ± 1.0 ka [*Guérin*, 1983]. The flow was sampled at several outcrops around the crater's perimeter. The paleomagnetic directions suggest that some of the outcrops might have been displaced after remanence acquisition, because, in spite of clustered directions of individual outcrops, there is a dispersion of the mean stable directions of several outcrops in the crater (Figure 3). This might have been caused by slumping of the outcrops, which line the crater rim and dip about 40° toward its center. We consider the stable remanence of each outcrop to have been acquired at the same instant.

Six samples were selected for paleointensity experiments, and results from five of them are listed in Table 1. The samples are from three outcrops of the Côme crater, and they were studied in two separate experiments (three specimens per experiment), performed with laboratory fields of 40 and 50 μT, respectively. The rock was a highly oxidized red scoria. Microscopic observations indicated that the magnetic minerals were highly oxidized titanomagnetites subdivided by ilmenite lamellae with inclusions of rutile rods (Figure 4), corresponding to the oxidation

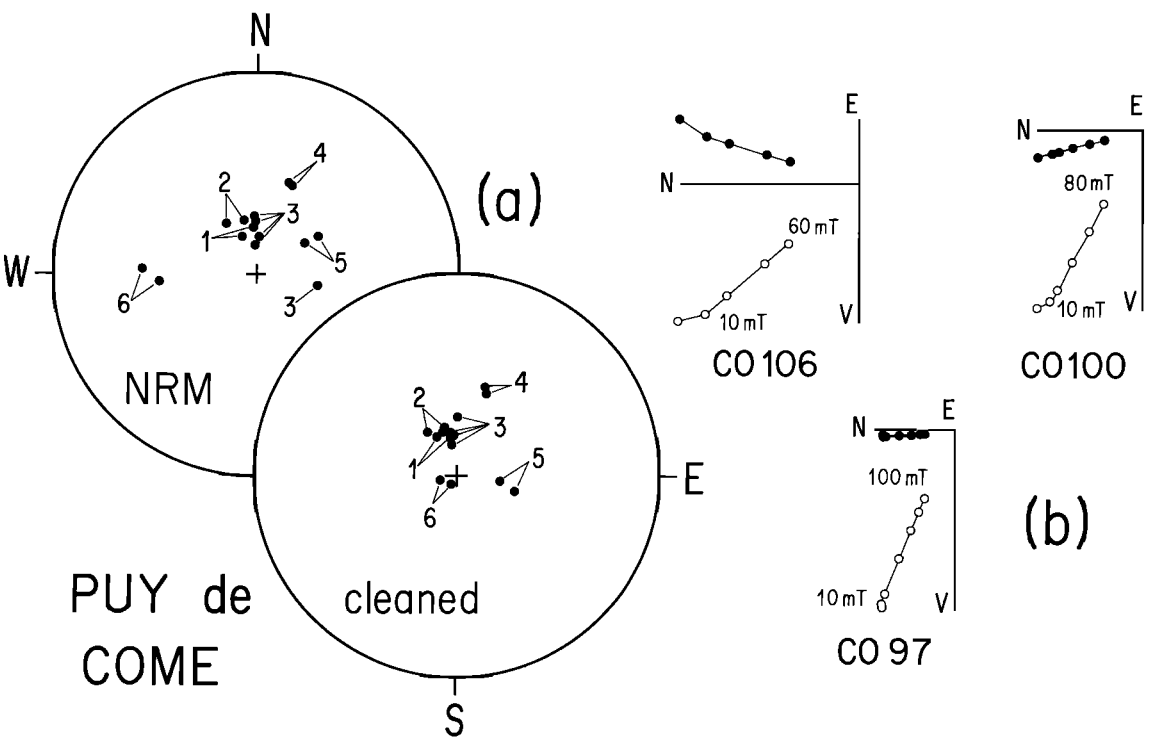

Fig. 3. (*a*) Paleomagnetic directions in the Puy de Côme crater. The numbers correspond to the different outcrops. Certain outcrops retain anomalous directions after AF cleaning. Each point represents a specimen from independently oriented cores, all with lower hemisphere directions. (*b*) Orthogonal projections of typical remanence vectors during AF demagnetization. Solid symbols, horizontal component; open symbols, projection on a vertical plane.

TABLE 1. Paleointensity Results From All Volcanic Flows

	No.	H_{lab}	A/V	n	T1	T2	b	σ	f	g	q	F
CO	97	40	A	12	200	560	-0.725	0.025	0.746	0.893	19.4	29.0
	98	50	A	15	100	550	-0.593	0.016	0.713	0.876	22.8	19.7
	103	40	A	12	200	560	-0.606	0.029	0.289	0.889	5.3	24.2
	104	40	A	12	200	560	-0.787	0.016	0.638	0.892	28.2	31.5
	105	50	A	15	100	550	-0.674	0.020	0.448	0.876	13.0	33.7
GO	87	40	A	7	200	490	-1.047	0.041	0.563	0.787	11.4	41.9
	93	50	A	15	100	550	-0.930	0.021	0.899	0.859	35.0	46.5
	94A	50	A	8	330	550	-0.973	0.043	0.850	0.826	16.0	48.6
	94B	40	A	8	330	540	-1.096	0.059	0.835	0.814	12.7	43.9
	95	50	A	15	100	550	-0.932	0.025	0.907	0.863	28.9	46.6
SA	165C	50	V	9	103	323	-1.165	0.076	0.535	0.766	6.3	58.3
	166	50	V	6	103	225	-1.214	0.090	0.631	0.628	5.4	60.7
CA	300	50	V	12	100	490	-1.216	0.044	0.262	0.794	5.7	60.8
	301	75	V	8	390	545	-0.829	0.019	0.577	0.775	20.0	62.2
	302	75	V	8	200	515	-0.906	0.044	0.367	0.825	6.2	67.9
PR	312	50	V	10	100	390	-1.426	0.050	0.211	0.869	5.2	71.3
	315	50	V	4	350	490	-1.352	0.059	0.274	0.618	3.9	67.6
NU	128C	40	V	10	200	540	-0.924	0.020	0.775	0.803	29.0	37.0
	128B	75	V	12	200	555	-0.464	0.009	0.841	0.865	36.2	34.8
	134C	40	V	11	200	550	-0.864	0.020	0.911	0.858	33.9	34.6
	134A	75	V	6	200	435	-0.627	0.040	0.205	0.728	2.3	42.7
PO	226	40	V	7	200	490	-0.810	-0.058	0.431	0.806	4.9	32.4
	227	50	V	5	240	490	-0.641	0.020	0.318	0.683	7.2	32.1
	228	50	V	8	240	550	-0.644	0.013	0.728	0.781	28.3	32.2
	229	40	V	8	200	520	-0.756	0.040	0.331	0.772	4.8	30.2
	231	50	V	5	240	490	-0.735	0.021	0.466	0.729	12.2	36.7
	204	20	V	9	250	540	-1.344	0.072	0.678	0.819	10.4	26.9
	206	20	V	8	250	530	-1.501	0.106	0.060	0.825	7.0	30.0
BAc	314	30	A	8	200	550	-1.150	0.027	0.938	0.381	15.5	34.5
	315	50	V	12	250	563	-0.656	0.012	0.821	0.877	40.1	32.8
	321	30	A	9	200	570	-1.160	0.040	0.893	0.816	21.3	34.8
	326	50	V	8	250	550	-0.497	0.024	0.455	0.650	6.2	25.9
BAuf	511B	30	V	5	250	470	-0.826	0.068	0.384	0.614	2.9	24.8
	511C	30	V	5	250	470	-0.960	0.130	0.397	0.659	1.9	28.8
	513	20	V	8	250	510	-1.326	0.078	0.861	0.820	12.0	26.5
	547	20	V	11	250	560	-1.445	0.029	0.817	0.867	35.8	28.9

No., sample number; H_{lab}, laboratory field intensity (μT); A/V, heating conducted in air (A) or vacuum (V); n, number of points used in the slope calculation; T1-T2, temperature range of slope calculation; b, slope of the straight line; σ, standard error of the slope; f, NRM fraction used in the calculation; g, between points gap factor; q, quality factor (f, g, q were defined by *Coe et al.* [1978]); F, paleointensity (μT).

state 3 or 4 of *Ade Hall et al.* [1968], summarized by *Johnson* [1978]. The J_s-T analyses (Figure 5) support the microscopic observations, showing a single magnetic component with a high Curie point and nearly reversible magnetization curves, which indicate high oxidation. Therefore the Thellier procedure was conducted in air at atmospheric pressure. Most of the treated specimens exhibited nearly ideal linear NRM-TRM behavior with straight-line segments defined by as many as 12–15 points, and the PTRM checks show no significant chemical change of the magnetic minerals on heating. (The PTRM checks are represented on the diagrams by arrows joining the double heating step, immediately prior to the check and the new PTRM at a lower temperature, which had been previously thermally demagnetized. Alteration of the magnetic properties would cause the arrow to deviate from the original PTRM.) The orthogonal vector projections of the thermal demagnetizations of these samples indicate a stable, single-component primary remanence. Typical examples of such behavior are shown in Figure 6. Sample CO 103 (Table 1) has a low quality factor because of the small fraction of demagnetized NRM (30% at 560°C) involved in the calculation. Hematite seems to be responsible for a significant remanence fraction in this sample, and further heatings would be required for a more complete thermal demagnetization. One sample was rejected because of a secondary overprint of the magnetization.

The similar paleointensity of samples from Puy de Côme is consistent with the inference that the different outcrops recorded the same paleofield. The mean paleointensity of the Puy de Côme crater unit is 30 ± 4 μT.

Pariou Flow

The second unit is the upper flow of the Puy de Pariou crater (GO), with a TL age of 8.1 ± 0.8 ka [*Guérin*, 1983]. This is in agreement with the ^{14}C date obtained on a nonburnt fossil pine wood under the flow [*Delibrias et al.*, 1964] which fixes its maximum age at about 9.4 ± 0.4 ka, after dendrochronological

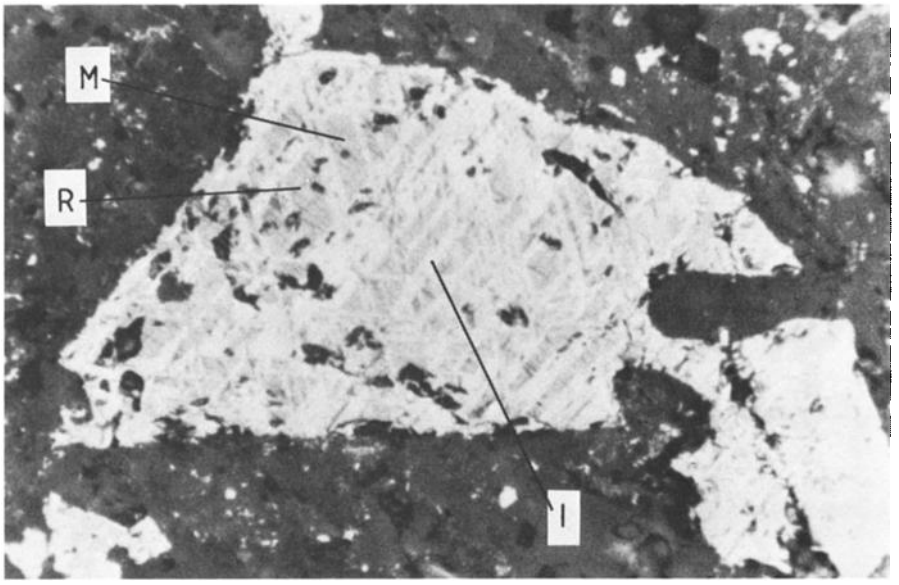

Fig. 4. Highly oxidized titanomagnetite from a scoria of the Puy de Come crater. M, residual magnetite; I,: ilmenite lamellae along the (111) planes of the host mineral; R, rutile rods. Oxidation state 3–4. Mineral length, 200 μm.

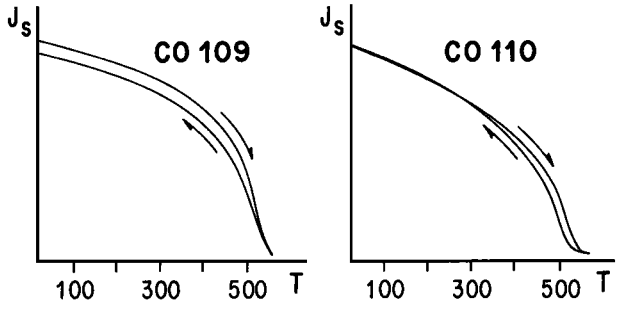

Fig. 5. High field saturation magnetization versus temperature (J_s-T) curves for the Puy de Côme samples. Experiments were performed in vacuum. Field intensity was 0.15 T. The arrows indicate heating and cooling. Temperatures are in degrees Celsius.

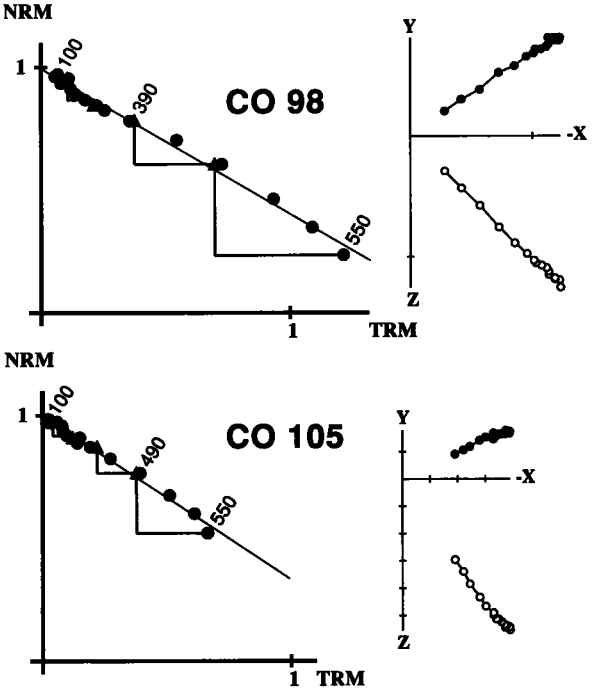

Fig. 6. Example of "good" NRM-TRM diagrams with corresponding evolution of the orthogonal vector projections of the remanence during thermal demagnetization in sample coordinates. No secondary component appears to exist. In the NRM-TRM plot solid symbols are points used for the paleointensity calculation, and the numbers refer to temperature steps in degrees Celsius.

correction. We sampled a scoria at the top of the flow. Although less oxidized than at the Puy de Côme, the minerals of this scoria are sufficiently oxidized, as indicated by the J_s-T curves (Figure 7), to conduct the Thellier experiments in air. Six specimens were selected and studied during two paleointensity experiments with laboratory fields of 40 and 50 μT, respectively; the results are listed in Table 1. Only five of the six samples gave reliable paleointensity results. (The results from the rejected specimen are shown in Figure 2*b*.) For core GO 94 we analyzed two specimens with small secondary components, which had only a minor influence on the NRM direction but caused a concave up curvature during the Thellier experiment and lead to an overestimate of the paleointensity. Hence we omitted from the paleointensity calculations data from temperatures below 330°C. For sample GO 87 (Figure 8) a positive PTRM check at 410°C was obtained after the heating step to 520°C. However, chemical alterations were indicated by the negative PTRM test at temperatures above 520°C, and it is evident that 520°C point is to the right of the straight line. This unit provides a reliable paleointensity of 46 ± 3 μT, similar to the present field.

Saint Saturnin Flow

The Saint Saturnin flow originated from the volcanic system of the vulcanoes La Vache-Lassolas. This flow has a ^{14}C age of 8.5 ± 0.4 ka. We sampled this flow at three sites, dated by the TL method [*Guérin*, 1983]. Two of the sites are known to belong to

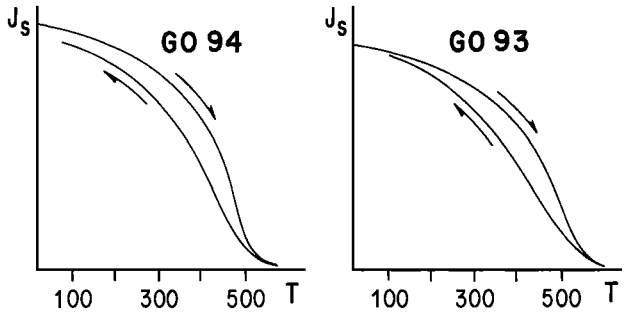

Fig. 7. J_s-T curves for samples from the Pariou flow. Experiments were performed in vacuum with an applied field of 0.5 T. Temperatures are in degrees Celsius.

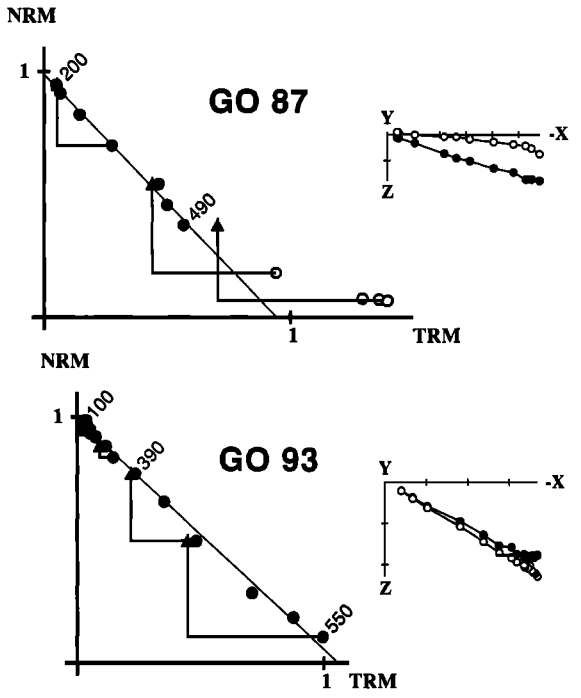

Fig. 8. Examples of NRM-TRM diagrams and the corresponding orthogonal vector projections of the remanence for the Pariou flow. In the NRM-TRM plot, open symbols indicate rejected points and solid symbols are points used for the paleointensity calculation. Other symbols are described in the captions of Figures 2 and 6.

TABLE 2. Paleomagnetic Results of the Saint Saturnin Flow

Site	D	I	n	k	α_{95}
SA	356.9	54.7	6	642	2.6
PR	0.5	55.8	8	152	4.5
CA	0.8	56.3	4	251	5.8
Mean	359.3	55.5	18	245	2.2

D, I, α_{95}, all in degrees, are the declination, inclination, and radius of 95% cone of confidence, respectively, of the mean direction; k, precision parameter of the Fisher distribution; n, number of cores measured.

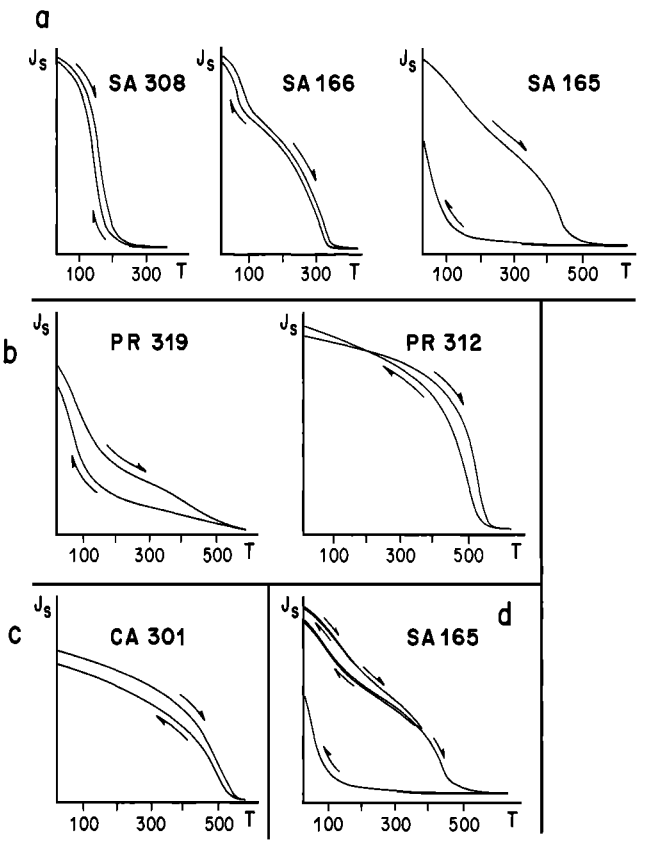

Fig. 9. (*a*) Varied thermomagnetic behavior for SA site. The third curve was observed for only one sample. (*b*) J_s-T behavior observed for PR site. (*c*) Typical J_s-T behavior of samples from CA site. (*d*) Progressive thermomagnetic experiment for different temperature ranges. No change occurs below 200°C; a slight change occurs between 200° and 390°C; this change is achieved for the last cooling. The applied field was 0.6 T. J_s-T experiments were done in vaccuum.

the same volcanic unit, and both TL ages are very similar to the ^{14}C age (SA, 8.8 ± 0.9 ka; CA, 9.2 ± 0.6 ka); however, the third site has a very different TL age (PR, 15.5 ± 1.7 ka). *Guérin* [1983] interpreted the older age of the PR site to suggest that it represents an islet of an older flow appearing in a window of the main Saint Saturnin flow. However, our paleomagnetic results suggest that all three sites belong to the same unit, which recorded the same paleomagnetic field. First, the paleomagnetic directions of the three sites are statistically indistinguishable (Table 2). Second, as we shall show below, the same paleointensity was obtained for the three sites, with differences not exceeding experimental errors. Furthermore, the mean paleointensity is not common for the interval 5–10 ka; rather, it corresponds to a maximum value of the geomagnetic field for Europe around 9 ka [*Bucha*, 1967; *Schweitzer and Soffel*, 1980]. Third, the petrography of the rocks at the three sites is similar, and they are tentatively characterized as olvine and pyroxene basalt. However, further petrographic analyses are required to strengthen this conclusion.

On the other hand, the magnetic mineralogy is considerably more varied and complex. For example, site SA exhibits reversible J_s-T curves of a single phase with a single low Curie temperature ($T_c \approx 200$°C), as well as irreversible two phase J_s-T curves (Figure 9*a*). The former behavior suggests the presence of stoichiometric magnetic minerals, probably unoxidized titanomagnetites, as indicated by the X ray analysis and microscopic observations (Figure 10). The two-phase behavior

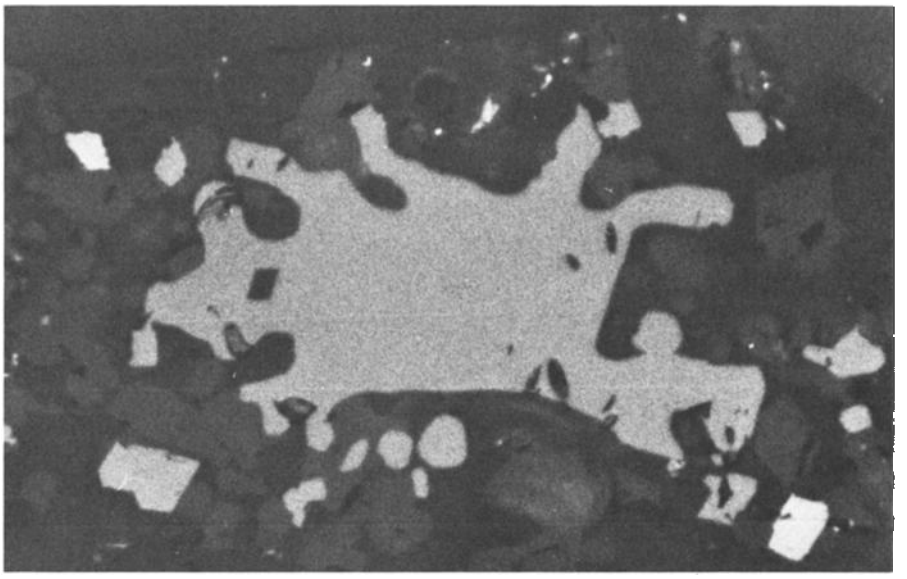

Fig. 10. Unaltered stochiometric titanomagnetite. Mineral length, 190 μm.

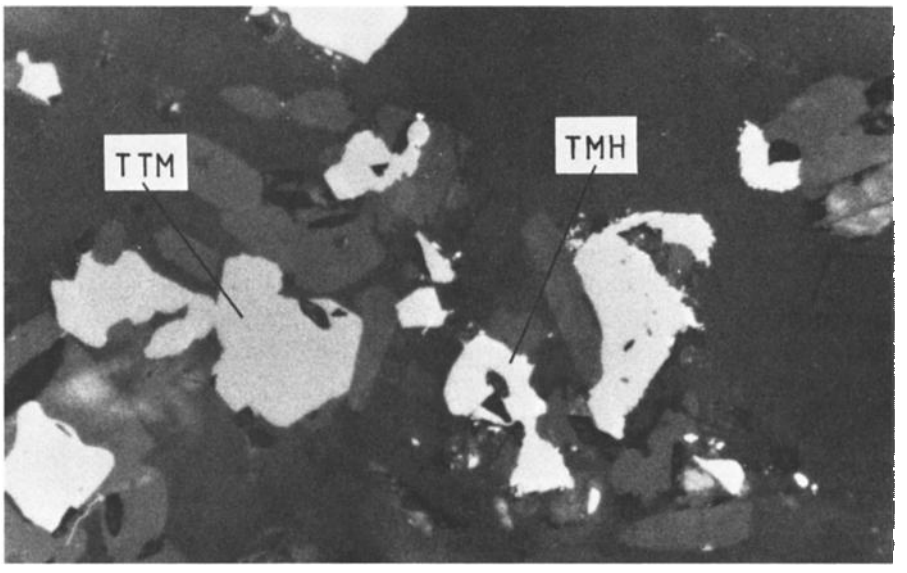

Fig. 11. Two kinds of magnetic minerals in the same sample. TTM, unaltered titanomagnetite; TMH, lightly oxidized titanomaghemite.

might be characteristic of the same mineral as above, which had undergone partial low-temperature oxidation to titanomaghemite (Figure 11), and is unstable at higher temperatures. At site PR we observed two-phase thermomagnetic behavior, as well as J_s-T curves with single high Curie temperature around 500°C (Figure 9*b*). The samples from site CA only had single high Curie points and reversible J_s-T surves (Figure 9*c*). Al samples with high Curie temperature also had relatively high MDFs $\gtrsim$ 30 mT, which are often associated with oxidized titanomagnetite (Figure 12). Samples with low Curie points usually had low MDF $\lesssim$ 15 mT. Specimens with more oxidized titanomagnetites and higher Curie points and MDFs are more suitable for paleointensity studies. However, it was desirable to obtain paleointensities from all three Saint Saturnin sites. In Figure 9*d* we show repeated thermomagnetic experiments to progressively higher temperatures to determine the temperature to which a sample can be heated without undergoing significant changes of its magnetic properties. For sample SA165C (Figure 9*d*) it appears that there are no significant changes below 210°C, with minor alteration occurring between 210° and 390°C. Therefore paleointensity experiments for these samples were done at low temperatures. Paleointensity results were obtained for two specimens from site SA. Data from four additional specimens at this site were rejected because of nonideal behavior. In general, the quality factors for this flow are rather low (Table 1). The samples from site PR have relatively reversible thermomagnetic curves; however, their magnetic properties were modified at intermediate temperatures after only a small part of the NRM was demagnetized, and the paleointensity

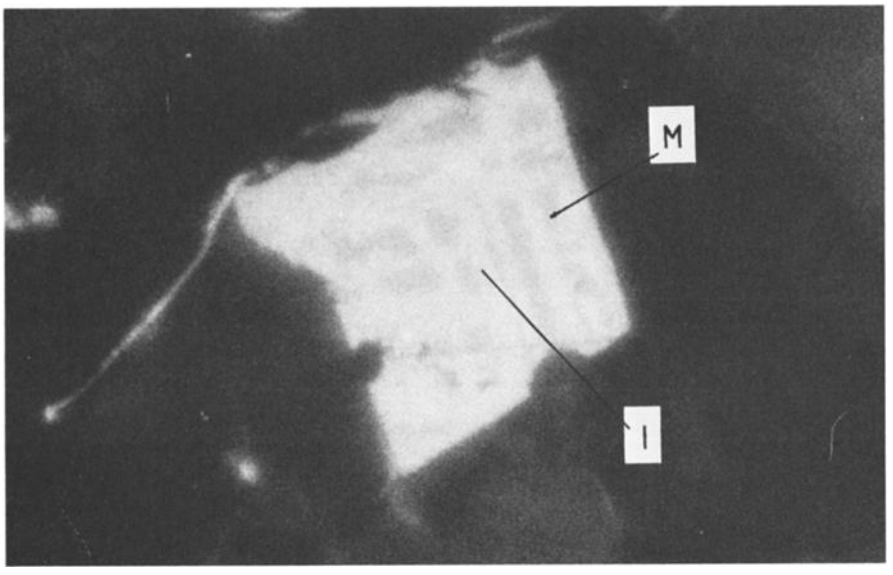

Fig. 12. Oxidized titanomagnetite, state 2. M, residual magnetite; I, ilmenite lamellae. Mineral size, 25 μm.

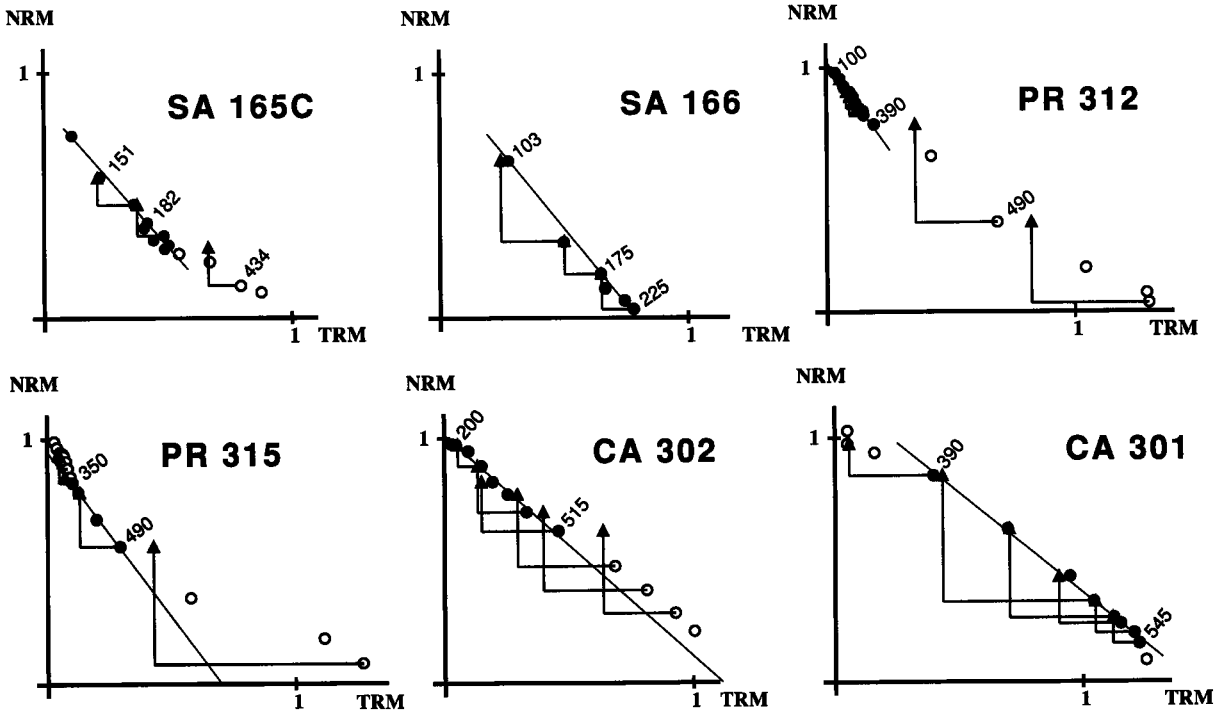

Fig. 13. NRM-TRM diagrams for samples from the three sites of the Saint Saturnin flow (SA, PR, CA). Symbols are described in the captions of Figures 2 and 6.

determinations are based on a small NRM fraction. In addition, one of the PR samples (PR 315) was overprinted by a secondary remanence with low blocking temperatures (Figure 13). Only site CA provided paleointensity determinations with higher q values, in spite of minor effects due to secondary remanence and chemical changes (Figure 13). Sample CA 300 shattered during the experiment, and no data were obtained for temperatures above 490°C. Although the q values of individual specimens are low, the paleointensity results for the Saint Saturnin flow are consistent and high (Table 1). The values of site PR show a slightly higher paleointensity than at the two other sites, but the differences are not significant, because the between-site dispersions are comparable to those that occur within sites.

When our results are compared with the European data [*Barton et al.*, 1979; *McElhinny and Senanayake*, 1982], the Saint Saturnin value represents an unusual high intensity which appeared just twice since 10 ka, at about 2.5 ka and 9 ka. The TL age of site PR is 15.5 ± 1.7 ka; however, paleointensities of Massif Central sites with ages between 10 and 40 ka [*Salis*, 1987] do not show such high values. Therefore we prefer the

interpretation that the three sites represent the same volcanic flow with an age of about 8.5 ka. The rather high mean paleointensity obtained for the Saint Saturnin flow 64 ± 5 μT is in good agreement with the results obtained for the same flow by *Barbetti and Flude* [1979] on baked sediments at site SA ($n = 5$, $H = 79 \pm 14$ μT). The results from this flow have a relatively small standard deviation, in spite of the low quality of individual determinations. In addition, the data from samples with various magnetic mineralogies and from separate sites provide a strong consistency argument for the paleointensity determined for the Saint Saturnin flow.

In order to obtain reliable paleointensities for difficult units, such as the Saint Saturnin flow, it is necessary to be equally stubborn and to be prepared to analyze more samples until one obtains a reliable estimate of the paleofield intensity. For this flow, 12 samples were studied, and seven produced usable results.

Nugère Flow

We also studied three units just older than 10 ka. The first is a vesicular andesite flow from the volcano La Nugère (NU), whose TL age is 10.9 ± 1.2 ka [*Guérin*, 1983]. The magnetic minerals show signs of relatively high-temperature oxidation having titanomagnetite grains with ilmenite lamellae (oxidation state 3). We chose samples with high Curie temperature (Figure 14), but it was difficult to find samples with reversible J_s-T curves. In two distinct paleointensity experiments the selected specimens with irreversible J_s-T curves did not provide successful results, either because of thermal changes upon heating or nonideal behavior due to multidomain grains. Specimens from only two cores showed "good" Thellier behavior, so we studied a second specimen from each of these cores, using different laboratory fields (40 and 75 μT). The four specimens gave consistent paleointensity values (Figure 15 and Table 1), and because we used different applied laboratory fields, the specimens were treated independently in calculating the mean paleointensity of 35.0 ± 1.2 μT. This flow was studied by *Thellier and Thellier* [1959], who measured six specimens and obtained a paleointensity of 33.5 ± 9.6 μT.

Pontgibaud Flow

The vesicular basaltic flow from the Puy de Côme volcano, was sampled at Pontgibaud (PO), and it was dated by TL as 11.6 ± 0.8 ka [*Guérin*, 1983]. The magnetic minerals are oxidized titanomagnetites with high Curie points ~540°C and frequently with nearly reversible J_s-T curves (Figure 16). Only samples with reversible J_s-T curves and high MDF were selected for the paleointensity experiments. CRM affects sample PO 226 above 490°C as noted on the demagnetization diagram (Figure 17).

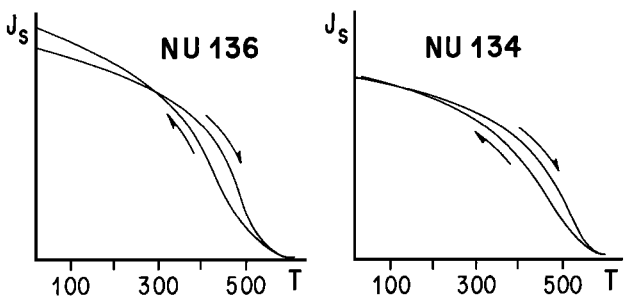

Fig. 14. J_s-T curves, for the Nugère flow samples. Experiments were performed in vacuum. Applied field, 0.5 T. Temperatures are in degrees Celsius.

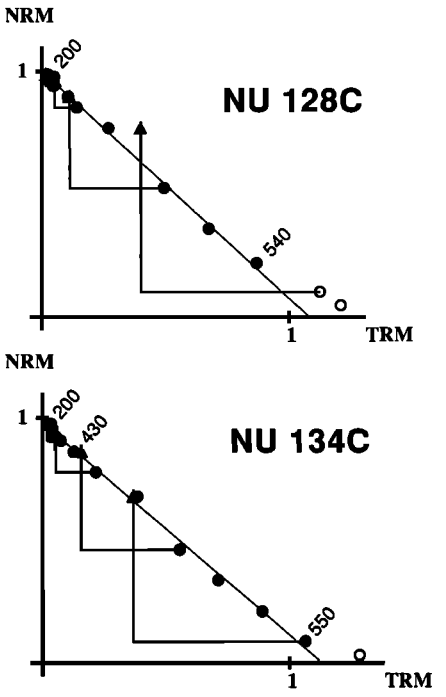

Fig. 15. Examples of NRM-TRM diagrams from the Nugère flow. Symbols are described in the captions of Figures 2 and 6.

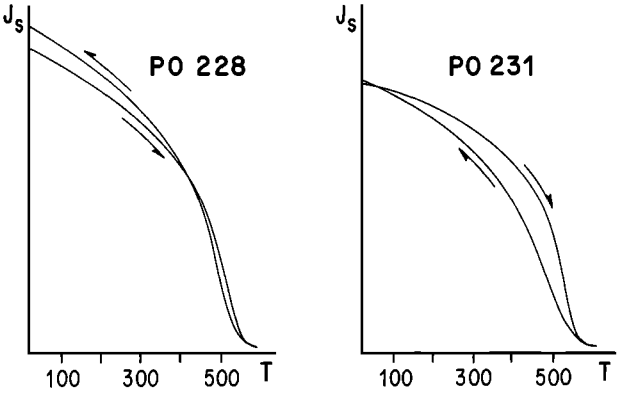

Fig. 16. J_s-T curves for samples from the Pontgibaud flow, showing high Curie temperatures and reversible behavior. Experiments were performed in vacuum. Applied field 0.5 T. Temperatures are in degrees Celsius.

However, linear NRM-TRM behavior and successful PTRM checks persisted to 550°C. The occurrence of linear (ideal) NRM-TRM plots in the presence of magnetochemical changes observed by thermal demagnetization, has been previously noted [e.g., *Prévot et al.*, 1983], and it reinforces the importance of simultaneously scrutinizing NRM-TRM data, PTRM checks, as well as thermal demagnetization results in selecting temperature steps for the paleointensity determinations. Except for specimen PO 228, all PO samples underwent some chemical change(s) near 500°C. However, at lower temperatures, consistent paleointensity results were obtained. The data for the Pontgibaud flow are listed in Table 1. (The last two specimens are from a different site of this flow.) The data are consistent, and the weighted mean paleointensity is 33.2 μT.

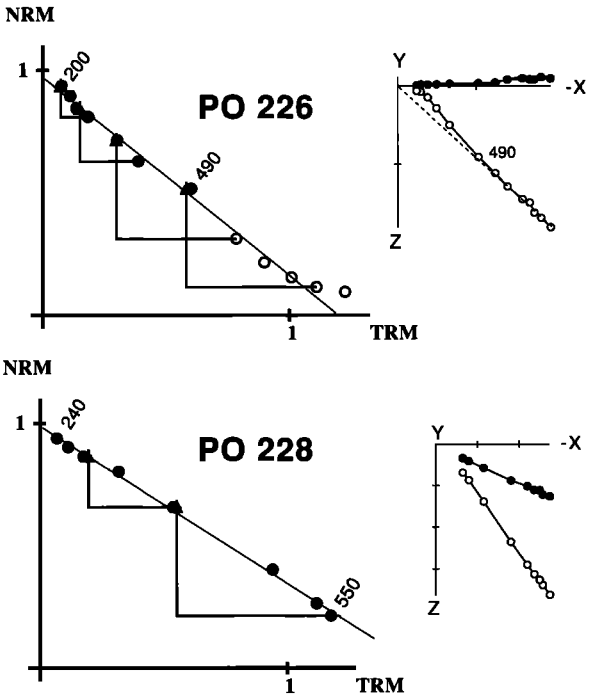

Fig. 17. Examples of NRM-TRM diagrams for the Pontgibaud flow. The dashed line on the orthogonal remanence projection illustrates the deviation of the direction toward the applied field, which was vertical up. Symbols are described in the captions of Figures 2 and 6.

Barme

The last unit of this study was from the Puys de Barme craters (BAc) and the upper flow of this volcano system (BAuf) (Figure 18). The paleomagnetic directions of these two sites are indistinguishable [*Bonhommet*, 1972], and it has been assumed that they recorded the same paleomagnetic field. One TL date was obtained for a sample from the upper flow with an age of 11.9 ± 1.2 ka [*Guérin*, 1983]. We sampled red scoria at the craters site and dark scoria from the upper flow; both sites are highly oxidized. For samples from the craters, two paleointensity determinations were done in air and two in vacuum (Table 1, BAc), and the paleointensities obtained in air are slightly higher than those in vacuum, but the differences remain well within the scatter of some sites. The difference in the paleointensities might be caused by oxidation of the magnetic minerals heated in air, shown as slight concave down curvature of the NRM-TRM diagram (Figure 19). However, such oxidation was not supported by PTRM checks, and at present the small differences between the paleointensity determinations in air and in va-cuum are not considered to be significant. The combined paleointensity of the two Barme sites (BAc and BAuf) has a weighted mean value of 30.9 μT.

DISCUSSION

Paleointensity Determinations

It is apparent from our results and the associated quality factors that the reliability of paleointensity determinations varies considerably between and even within individual units. In our experiments, the best rock type for paleointensity determinations seems to be highly oxidized scoria, which usually give reliable results even when heated in air. Among the flows, vesicular units

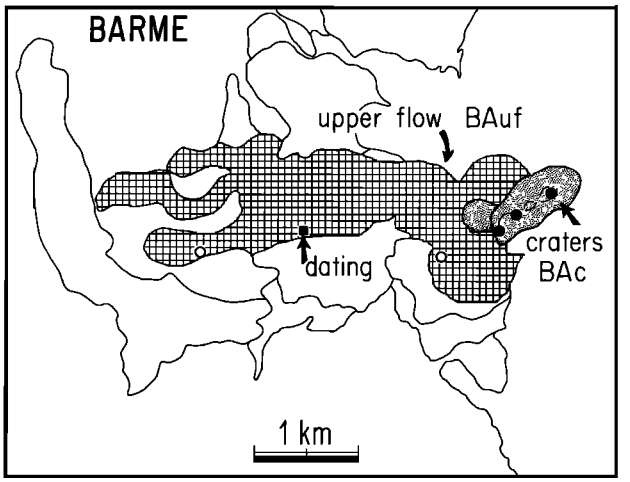

Fig. 18. Location of the studied Barme units. The solid circles represent sites from the crater scoria; the open circles are sites on the upper flow; the square denotes the location of the dated sample from the upper flow.

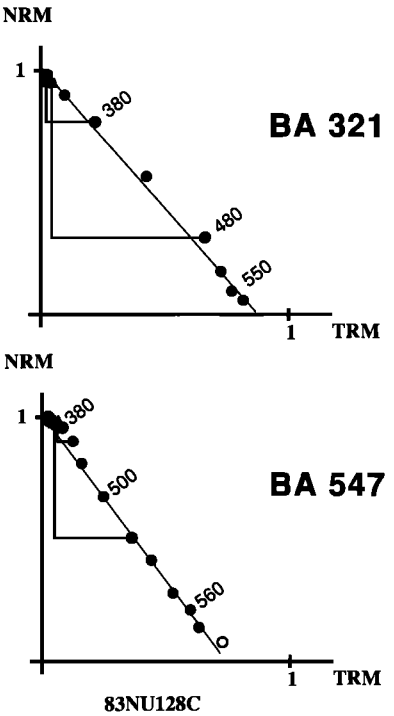

Fig. 19. NRM-TRM diagrams from Barme units. Symbols are described in the captions of Figures 2 and 6.

are often good candidates for paleointensity studies, especially if their magnetic minerals are highly oxidized, because then they are less susceptible to chemical changes during subsequent laboratory heatings. Such samples are most likely to satisfy the sample selection criteria of having high Curie temperatures, reversible J_s-T curves, and high MDFs. When dealing with units such as the massive Saint Saturnin flow, where these criteria are not met, it might still be possible to determine the paleointensity by using more complete information about the thermomagnetic behavior; in these cases the quality of the data is usually lower, and relatively more samples need to be measured, because of a higher ratio of unsuccessful determinations.

TABLE 3. Paleomagnetic Vectors of Studied Units

Unit	Ages,	Stable Directions					Paleointensities				
	ka	n	D	I	k	α_{95}	n_I	$F_m \pm$sd	F_w	VADM	VDM
Côme (CO)	7.6±1.0	9	350.0	65.1	211	3.6	5	29.6±3.5	30.2	4.9	4.8
Pariou,(GO)	8.1±0.8	13	351.6	69.7	221	2.8	5	45.5±2.6	45.9	7.5	6.9
S. Saturnin	8.5±0.4	18	359.3	55.5	245	2.2	7	64.1±4.8	63.8	10.4	11.6
Nugère (NU)	10.9±1.2	9	326.2	66.2	414	2.5	4	37.2±3.8	35.8	5.8	5.6
Pontgibaud (PO)	11.6±0.8	9	351.2	60.8	796	1.8	7	32.7±2.4	33.2	5.3	5.6
Barme (BA)	11.9±1.2	9	29.8	49.1	224	3.4	8	29.6±3.9	30.9	5.0	6.0

Ages are by TL method *[Guérin, 1983]*, except ^{14}C date for the Saint Saturnin flow; n (n_I), number of samples used for average paleomagnetic directions (intensities); D, I, α_{95}, all in degrees, the declination, inclination, and radius of 95% cone of confidence, respectively, of the mean direction; k, precision parameter of Fisher distribution; F_m, arithmetic mean paleointensity and standard deviation; F_w, weighted mean paleointensity following *Prévot et al.* [1985]; all field values are in microtesla (μT); VDM (VADM), virtual (axial) dipole moment ($\times 10^{22}$ A m^2).

Table 3 shows the paleomagnetic vectors of the studied units, including their directions and magnitudes. The weighted mean of each unit is considered to represent the best estimate of the paleointensity. The arithmetic mean paleointensity and its associated standard deviation are listed to emphasize the intraunit dispersion. The weighted and arithmetic mean paleointensity are very similar for each of the units studied.

The individual q factors were used to weight the paleointensity of each sample in calculating the mean paleointensity for every lava. In analyzing the NRM-TRM data, careful judgement must be exercised so that maximizing q does not become a goal in itself. In this study there were several samples, where subtle increases in the PTRM capacity at higher temperatures was detected by PTRM checks, although the NRM-TRM data were linear for most of the blocking temperature range. The use of the linearity of the NRM-TRM points as the primary criterion for calculating the paleointensity would have favored including certain higher temperature points (leading to higher q values), which were precluded on the basis of PTRM checks. Thus higher q values due to longer linear segments of NRM-TRM data might contain systematic errors and yield less correct paleointensities.

Paleointensity Variation in the Holocene

The paleointensity of each unit represents the magnitude of the total geomagnetic field at the site and time of remanence acquisition, including dipole and nondipole contributions. To compare our results with existing data from around the world for the Holocene, the paleointensity data were transformed to virtual dipole moment (VDM) and virtual axial dipole moment (VADM), the dipole and axial dipole magnitudes that would produce the observed field intensity and inclination at the sampling site [see *Barton et al.*, 1979]. This representation enables comparisons of data from different latitudes and does not introduce scatter arising from dipole wobble. In addition, averaging VDMs and VADMs over successive time intervals for different geographical regions would permit discrimination between some dipole and nondipole intensity fluctuations, especially where significant differences are observed in the patterns from different areas.

First, we compare our results with those for Europe, as analyzed by *McElhinny and Senanayake* [1982], who averaged data from different parts of Europe in intervals of 0.5 and 1.0 $\times 10^3$ years (Figure 20). Also plotted are the results from the present study in the Chaîne des Puys and from Iceland [*Schweitzer and Soffel*, 1980]. The paleointensities of the three younger units (Côme, Pariou, Saint Saturnin) and the Icelandic data fit very well with previous results, showing the pronounced decrease in intensity from 9 to 6.5 ka with a maximum VDM of 11.6 $\times 10^{22}$ A m^2 at approximately 9 ka, which had been previously observed for Czechoslovakia [*Bucha*, 1967]. The low paleointensity at about 7.5 ka with VDM value of 4.8 $\times 10^{22}$ A m^2 corresponds to the minimum in Figure 20, consistent with the quasi-sine paleointensity fluctuation for Europe since 10 ka with a period of 6–7 $\times 10^3$ years.

The older units of this study (Nugère, Pontgibaud, Barme) extend the data for Europe beyond 10 ka. The TL ages of these lavas are from 10.9 to 11.9 ka with about 10% uncertainty for each date, and they have similar and low paleointensities with VDMs between 5 and 6 $\times 10^{22}$ A m^2. However, the dispersed paleomagnetic directions of these extrusives (Table 3) indicate that they recorded different paleomagnetic vectors. Our results are supported by similar low VDM values for 10.5 ka flows from Iceland [*Schweitzer and Soffel*, 1980].

The vertical bars associated with the average VDMs from *McElhinny and Senanayake* [1982] represent the estimated standard deviation in each age interval. The differences between these

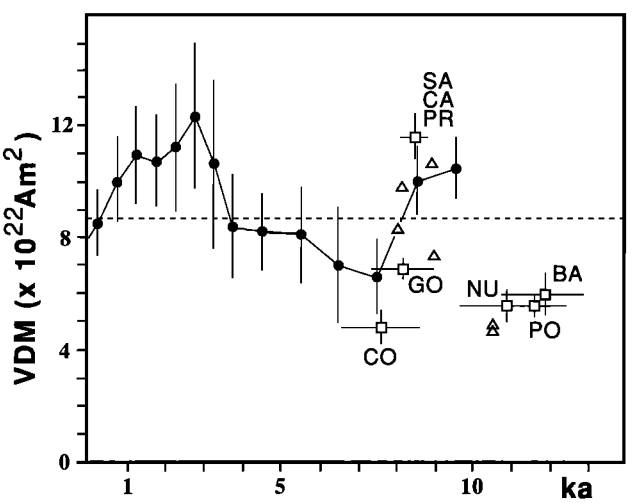

Fig. 20. VDM data for Europe since 12 ka. Solid circles are averages of published data through the 1970s, and the dashed horizontal line at 8.75 $\times$ 10^{22} A m^2 represents the average VDM since 10 ka from *McElhinny and Senanayake* [1982]. Open squares are results of the present study. Each intensity represents the weighted mean; the standard errors of the intensities are associated with the respective arithmetic means. Open triangles are results from Iceland [*Schweitzer and Soffel*, 1980].

average VDM values for Europe and the individual paleointensity results might be due to experimental errors, estimated at about 10% [*McFadden and McElhinny*, 1982], or rapid temporal and spatial variations of the geomagnetic intensity as well as about 10% dating uncertainty for each extrusive.

The scarcity of paleointensity data outside of Europe, especially prior to 4–5 ka, render any global generalizations as highly uncertain, and our attempts to do so are tentative indeed. The paleointensity high around 9 ka for Europe has now been confirmed by results from France, Iceland, and Czechoslovakia, supporting the quasi-sine VDM variation for Europe during the early Holocene and indicating the existence of a high paleointensity for about $1–2 \times 10^3$ year period at this time with VDM values 30% higher than the average since 10 ka (Table 3). Paleointensity measurements of dated lavas in Japan [*Tanaka*, 1980] provide additional evidence for high VADMs of $14–15 \times 10^{22}$ A m^2 between 8 and 10 ka, and *Coe et al.* [1978] reported a VADM of 10.0×10^{22} A m^2 for a Hawaiian lava dated at 10.4 ± 0.3 ka. Thus it is probably premature to reject the possibility that the $1–2 \times 10^3$ year duration high VDM at circa 9 ka is a rapid global fluctuation that reflects the behavior of the main geomagnetic field.

In Europe low VADMs from 10 to 12 ka were reported from France and Iceland with values about 30% below the average since 10 ka (Table 3). In addition, the three lavas from the western United States with ages between 10 and 12 ka also have VADM values less than the average since 10 ka [*Champion*, 1980], as is true for the two lavas from Hawaii with ages >10.4 and 17.9 ± 0.7 ka [*Coe et al.*, 1978] as well as a 13.8 ± 0.9 ka lava from Japan [*Tanaka*, 1980]. Thus, though sparse, the existing data suggest that the lower than average VADM from 10 to 12 ka might be a global feature of the main geomagnetic field.

Acknowledgments. The authors thank P. Roperch for many contributions at all stages of this study and on both sides of the Atlantic. Helpful comments by D. Champion, an anonymous reviewer, and an Associate Editor considerably improved this paper. S. Levi acknowledges support of the National Science Foundation.

REFERENCES

Ade Hall, J. M., M. A. Khan, P. Dagley, and R. L. Wilson, A detailed opaque petrological and magnetic investigation of a single Tertiary lava from Skye, Scotland, I, Iron-titanium oxide petrology, *Geophys. J. R. Astron. Soc.*, *16*, 375–388, 1968.

Aitken, M. J., A. L. Allsop, G. D. Bussel, and M. B. Winter, Geomagnetic intensity in Egypt and western Asia during the second millennium B.C., *Nature*, *310*, 305–306, 1984.

Aitken, M. J., A. L. Allsop, G. D. Bussel, and M. B. Winter, Greek archaeomagnitudes, *Nature*, *314*, 753, 1985.

Athavale, R. N., Intensity of the geomagnetic field in prehistoric Egypt, *Earth Planet. Sci. Lett.*, *8*, 221–224, 1969.

Barbetti, M., and K. Flude, Paleomagnetic field strengths from sediments baked by lava flows of the Chaîne des Puys, France, *Nature*, *278*, 153–155, 1979.

Barton, C. E., R. T. Merrill, and M. Barbetti, Intensity of the Earth's magnetic field over the last 10,000 years, *Phys. Earth Planet. Inter*, *20*, 96–110, 1979.

Bonhommet, N., Sur la direction d'aimantation des laves de la Chaîne des Puys, et le comportement du champ terrestre en France au cours de l'événement du Laschamp, thèse, Univ. of Strasbourg, Strasbourg, 1972.

Bucha, V., Archaeomagnetic and paleomagnetic study of the magnetic field of the earth in the past 600,000 years, *Nature*, *213*, 1005–1007, 1967.

Bucha, V., R. E. Taylor, R. Berger, and E. W. Haury, Geomagnetic intensity changes during the past 8500 years in the western hemisphere, *Science*, *168*, 111–114, 1970.

Champion, D. E., Holocene geomagnetic secular variation in the western United States: Implications for the global geomagnetic field, Ph.D. thesis, Calif. Inst. of Technol., Pasadena, 1980.

Coe, R. S., Paleointensities of the Earth's magnetic field determined from Tertiary and Quaternary rocks, *J. Geophys. Res.*, *72*, 3247–3262, 1967*a*.

Coe, R. S., The determination of paleo-intensities of the Earth's magnetic field with emphasis on mechanisms which could cause non-ideal behavior in Thellier's method, *J. Geomagn. Geoelectr.*, *19*, 157–179, 1967*b*.

Coe, R. S., and S. Gromme, A comparison of three methods of determining geomagnetic paleointensities, *J. Geomagn Geoelectr.*, *25*, 415–435, 1973.

Coe, R. S., S. Gromme, and E. A. Mankinen, Geomagnetic paleointensities from radiocarbon-dated lava flows on Hawaii and the question of the Pacific nondipole low, *J. Geophys. Res.*, *83*, 1740–1756, 1978.

Cox, A., Lengths of geomagnetic polarity intervals, *J. Geophys. Res.*, *73*, 3247–3260, 1968.

Delibrias, G., M. Y. Guillier, and J. Labeyrie, Saclay natural radiocarbon measurements, I, *Radiocarbon*, *6*, 238–239, 1964.

Games, K. P., The magnitude of the paleomagnetic field: A new non-thermal, non-detrital method using sun-dried bricks, *Geophys. J. R. Astron. Soc.*, *48*, 315–329, 1977.

Games, K. P., The magnitude of the archaeomagnetic field in Egypt between 3,000 and 0 B.C., *Geophys. J. R. Astron. Soc.*, *63*, 45–56, 1980.

Guérin, G., La thermoluminescence des plagioclases, Méthode de datation du volcanisme, Applications au domaine francais: Chaîne des Puys, Mont-Dore et Cézallier, Bas Vivarais, thèse, Univ. of Paris, Paris, 1983.

Johnson, H. P., Opaque mineralogy of the igneous rock samples from DSDP hole 395 A, *Initial Rep. Deep Sea Drill. Proj.*, *45*, 407–420, 1978.

Khodair, A. A., and R. S. Coe, Determination of geomagnetic paleointensities in vacuum, *Geophys. J. R Astron. Soc.*, *42*, 107–115, 1975.

Kitazawa, K., Intensity of the geomagnetic field in Japan for the past 10,000 years, *J. Geophys. Res.*, *75*, 7403–7411, 1970.

Kono, M., and H. Tanaka, Analysis of the Thellier's method of paleointensity determination, 1, Estimation of statistical errors, *J. Geomagn. Geoelectr.*, *36*, 267–284, 1984.

Kono, M., and H. Tanaka, Experimental errors in paleointensity determination, paper presented at IAGA 5th General Assembly, Prague, 1985.

Kovacheva, M., Summarized results of the archaeomagnetic investigation of the geomagnetic field variation for the last 8,000 years in southeastern Europe, *Geophys. J. R. Astron. Soc.*, *61*, 57–64, 1980.

Kovacheva, M., Archaeomagnetic investigations of geomagnetic secular variation, *Philos. Trans. R. Soc. London, Ser. A*, *306*, 79–86, 1982.

Kovacheva, M., and D. Veljovich, Geomagnetic field variations in southeastern Europe between 6,500 and 100 years B.C., *Earth Planet. Sci Lett.*, *37*, 131–138, 1977.

Levi, S., Comparison of two methods of performing the Thellier experiment (or, how the Thellier experiment should not be done), *J. Geomagn. Geoelectr.*, *27*, 245–255, 1975.

Levi, S., The effect of magnetite particle size on paleointensity determinations of the geomagnetic field, *Phys. Earth Planet. Inter.*, *13*, 245–259, 1977.

McElhinny, M. W., and W. E. Senanayake, Variations in the geomagnetic dipole, 1, The past 50,000 years, *J. Geomagn. Geoelectr.*, *34*, 39–51, 1982.

McFadden, P. L., and M. W. McElhinny, Variations in the geomagnetic dipole, 2, Statistical analysis of VDMs for the past 5 million years, *J. Geomagn. Geoelectr.*, *34*, 163–189, 1982.

Nagata, T., Y. Aray, and K. Momose, Secular variation of the geomagnetic total force during the last 5000 years, *J. Geophys. Res.*, *68*, 5277–5281, 1963.

Prévot, M., E. D. Mankinen, S. Gromme, and A. Lecaille, High paleointensities of the geomagnetic field from thermomagnetic studies on the rift valley pillow basalts from the Mid-Atlantic Ridge, *J. Geophys. Res.*, *88*, 2316–2326, 1983.

Prévot, J., E. A. Mankinen, R. S. Coe, and S. Gromme, The Steens Mountain (Oregon) geomagnetic polarity transition II. Field intensity variations and discussion of reversal models, *J. Geophys. Res.*, *90*, 10,417–10,448, 1985.

Salis, J. -S., Variation séculaire du champ magnétique terrestre.

Directions et paleointensités - sur la période 7000–70 000 ans BP, dans la Chaîne des Puys, *Thèses, Mémoires et documents du CAESS*, 190 pp., Rennes, 1987.

Schweitzer, C., and H. C. Soffel, Paleointensity measurements on postglacial lavas from Iceland, *J. Geophys.*, *47*, 57–60, 1980.

Sternberg, R. S., Archaeomagnetism in the Southwest of North America, in *Geomagnetism of Baked Clays and Recent Sediments*, edited by K. M. Creer, P. Tucholka, and C.E. Barton, pp. 158–167, Elsevier, Amsterdam, 1983.

Tanaka, H., Intensity variations of the geomagnetic field in Japan during the last 30,000 years, determined from volcanic rocks and potteries, Ph.D. thesis, Tokyo Inst. of Technol., Tokyo, 1980.

Thellier, E., and O. Thellier, Sur l'intensité du champ magnétique terrestre dans le passé historique et géologique, *Ann. Géophys.*, *15*, 285–376, 1959.

Walton, D., Geomagnetic intensity in Athens between 2,000 B.C. and A.D. 400, *Nature*, *277*, 643–644, 1979.

Walton, D., Re-evaluation of Greek archaeomagnitude, *Nature*, *310*, 740–743, 1984.

Williamson, J. H., Least-squares fitting of a straight line, *Can. J. Phys.*, *46*, 1845–1847, 1968.

York, D., Least-squares fitting of a straight line, *Can. J. Phys.*, *44*, 1079–1086, 1966.

York, D., The best isochron, *Earth Planet. Sci. Lett.*, *2*, 479–482, 1967.

N. Bonhommet and J.-S. Salis, Laboratoire de Géophysique Interne, Université de Rennes I, 35042 Rennes cédex, France.

S. Levi, College of Oceanography, Oregon State University, Corvallis, OR 97331.

(Received March 29, 1988;
revised May 1, 1989;
accepted May 25, 1989.)